Articles

Energetics of Hydrogen Bond Networks in RNA: Hydrogen Bonds Surrounding G+1 and U42 Are the Major Determinants for the Tertiary Structure Stability of the Hairpin Ribozyme†

Dagmar Klostermeier‡ and David P. Millar*

Department of Molecular Biology, The Scripps Research Institute, MB-19, 10550 North Torrey Pines Road, La Jolla, California 92037

Received January 14, 2002; Revised Manuscript Received September 9, 2002

ABSTRACT: The hairpin ribozyme, a small catalytic RNA consisting of two helix−loop−helix motifs, serves as a paradigm for RNA folding. In the active conformer, the ribozyme is docked into a compact structure via loop−loop interactions. The crystal structure of the docked hairpin ribozyme shows an intricate network of hydrogen bonding interactions at the docking interface, mediated by the base, sugar, and phosphate groups of U42 and G+1 [Rupert, P. B., and Ferre-D'Amare, A. R. (2001) *Nature 410*, 780−786]. To elucidate the determinants for tertiary structure stability in the hairpin ribozyme, we evaluated the energetic contributions of hydrogen bonds surrounding U42 and G+1 by time-resolved fluorescence resonance energy transfer using modified ribozymes that lack one or more of the individual interactions. Elimination of a single tertiary hydrogen bond consistently resulted in a net destabilization of ∼2 kJ/mol. The results of double- and triple-mutant cycles suggest that individual hydrogen bonds surrounding G+1 or U42 act cooperatively and form extended hydrogen bond networks that stabilize the docked ribozyme. These results demonstrate that RNAs, similar to proteins, can exploit coupled hydrogen bond networks to stabilize the docking of distant structural domains.

With a large number of RNA structures that have been determined, the molecular principles governing the architecture of RNA are beginning to emerge (reviewed in ref *1*). Helical regions can stack in an end-to-end fashion, or dock side by side. Interactions between distant parts of the molecules are mediated by common motifs, such as pseudoknots, loop−loop and loop−helix interactions, ribose zippers, and adenosine platforms.

The tobacco ringspot virus hairpin ribozyme, a small catalytic RNA motif required for processing satellite RNA replication intermediates (reviewed in ref *2*), consists of two helix−loop−helix elements on adjacent arms of a four-way helical junction (4WJ,[1] Figure 1A). In the catalytically active conformation, the ribozyme forms a compact, docked structure where the two loops interact (*3*−*6*). The crystal structure of the 4WJ hairpin ribozyme in the docked conformation (*7*) provides the first direct view of the docking interface, revealing a network of interactions between loops A and B.

Three sets of interactions may contribute to the tertiary structure stability of the hairpin ribozyme. First, a ribose zipper motif involving A10, G11, A24, and C25 connects the two loops via four hydrogen bonds. Second, the G+1 base adjacent to the cleavage site points into a pocket lined by A24, C25, G36, and A38 (loop B) and G8, A9, and A10 (loop A). G+1 forms various hydrogen bonds with the bases of G8, C25, and G36. Third, the U42 base from loop B packs into a pocket formed between the minor grooves of the A22·U41 and A23·A40 (loop B) and C−2·G11 and A−3·U12 (loop A) base pairs. U42 is engaged in hydrogen bonds with A22, A23, G11, and U12.

We recently probed the contributions of individual hydrogen bonds in the ribose zipper to the stability of the docked hairpin ribozyme using time-resolved fluorescence resonance energy transfer (trFRET) (*8*). Surprisingly, even though biochemical evidence for the ribose zipper interactions has been presented in the context of a minimal two-way junction ribozyme (*5*, *9*−*12*), elimination of the zipper only leads to a marginal destabilization of the docked four-way junction ribozyme (*8*). Consequently, the major determinants of the tertiary structure stability in the 4WJ hairpin ribozyme remain unknown. In an effort to understand the general principles of RNA tertiary structure stability, we investigated the energetic contributions of hydrogen bonds in the U42 and G+1 binding pockets by trFRET using modified ribozymes that lack one or more of the individual interactions.

† This work was supported by NIH Grant GM 58873 (to D.P.M.).

* To whom correspondence should be addressed. Phone: (858) 784-9870. Fax: (858) 784-9067. E-mail: millar@scripps.edu.

‡ Present address: Department of Experimental Physics, University of Bayreuth, Universitaetsstrasse 30, 95440 Bayreuth, Germany.

[1] Abbreviations: 2WJ and 4WJ, two-way and four-way helical junctions, respectively; Fl, fluorescein; TMR, tetramethylrhodamine; Pur, purine; I, inosine; 2-AP, 2-aminopurine; (tr)FRET, (time-resolved) fluorescence resonance energy transfer; ssFRET, steady-state fluorescence resonance energy transfer.

10.1021/bi025551b CCC: $22.00
Published on Web 11/06/2002

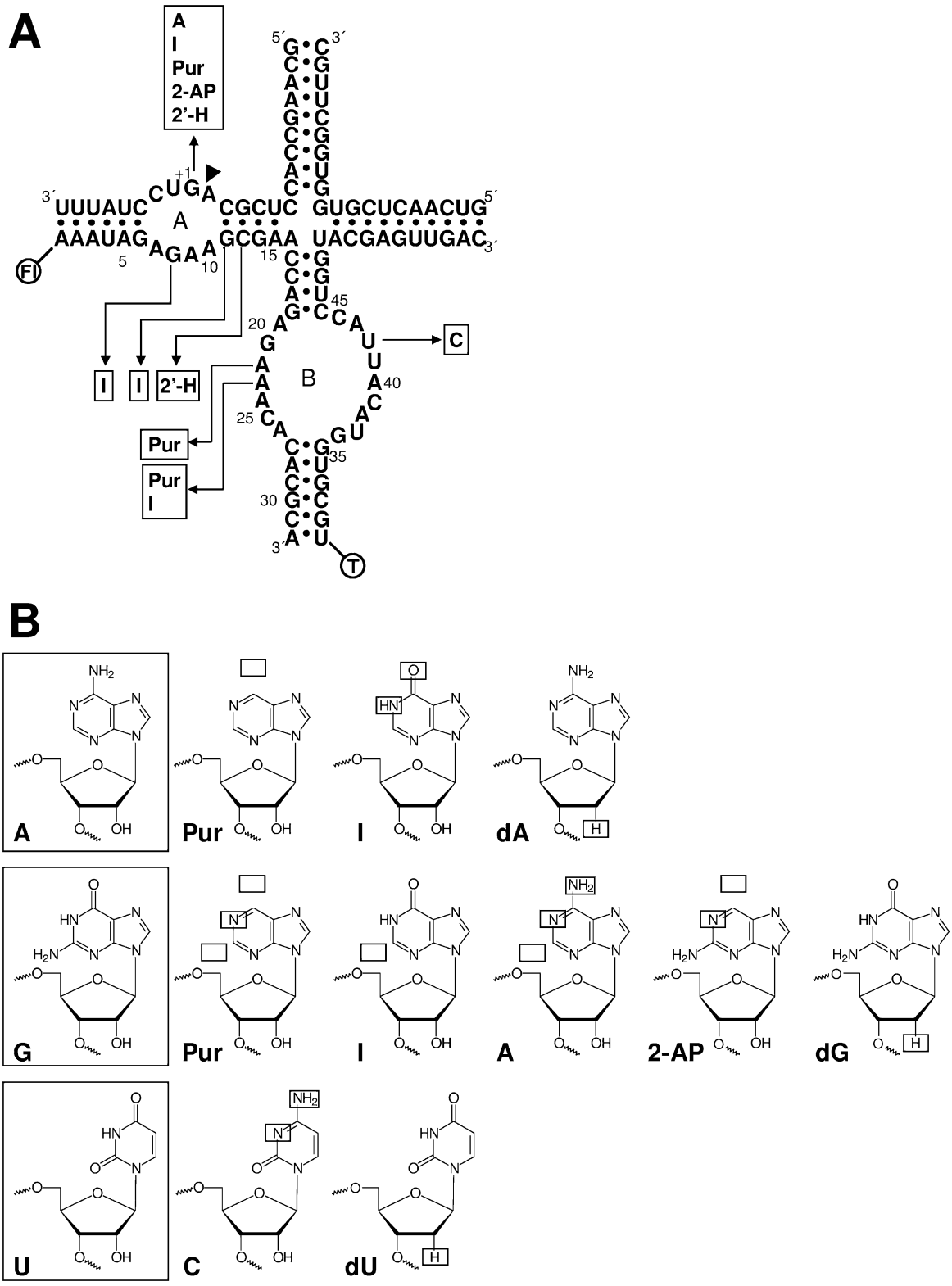

FIGURE 1: Construct and modifications that were used. (A) Ribozyme constructs. Fl and T refer to the fluorescein donor and tetramethylrhodamine acceptor dyes, respectively, separated from the RNA by six-atom linkers. Modifications were introduced into loop A (G8, G11, U12, and G+1) and loop B (A22, A23, and U42) as shown. Pur refers to purine and I to inosine; 2-AP is 2-aminopurine, and 2′-H denotes 2′-deoxy modifications. Note that this construct contains a C instead of a U at position 12. For purposes of consistency, it is referred to as U12 throughout the text. (B) Chemical structures of modified nucleotides. Chemical modifications relative to the wild type are highlighted with boxes. Replacing A with Pur eliminates the exocyclic amino group as a hydrogen bond donor, while substitution with I places a potential hydrogen bond acceptor in the 6 position, and changes the 1 position from a hydrogen bond acceptor to a donor. Substitution of G with Pur eliminates the exocyclic amino group as a hydrogen bond donor and the O6 as a hydrogen bond acceptor. Position 1 is changed from a hydrogen bond donor to an acceptor. I only eliminates the exocyclic amino group, while A lacks the exocyclic amino group and inverts positions 1 and 6 to hydrogen bond acceptor and donor, respectively. 2-AP retains the exocyclic amino group but eliminates O6 as a hydrogen bond acceptor and inverts position 1 to a hydrogen bond acceptor. Substitution of U with C places a potential hydrogen bond donor in the 4 position, and changes the 3 position from a hydrogen bond donor to an acceptor. 2′-Deoxy modifications eliminate the 2′-hydroxyl as a hydrogen bonding partner.

EXPERIMENTAL PROCEDURES

Preparation of RNA Samples. RNA strands were purchased from Dharmacon (Boulder, CO). The sequences were 5′-Fl-AAA UAG AGA AGC GAA CCA GAG AAA CAC ACG CA-3′, 5′-(TMR-)UGC GUG GUA CAU UAC CUG GUA CGA GUU GAC-3′, 5′-GUC AAC UCG UGG UGG CUU GC-3′, and 5′-GCA AGC CAC CUC GCdA GUC CUA UUU-3′. The deoxy modification at position −1 prevents cleavage. The following modifications were introduced, either singly or in various combinations: U42C, A23Pur, A23I, A22Pur, G11I, G+1A, G+1Pur, G+1−2-AP, G+1I, and G8I modifications were introduced, along with combinations thereof. The RNA was purified and annealed in 50 mM Tris-HCl (pH 7.5) and 12 mM $MgCl_2$ as described previously (*8*, *13*).

Time-Resolved Fluorescence Measurements and Data Analysis. Picosecond time-resolved donor emission profiles were collected using time-correlated single-photon counting. Pulsed excitation was achieved with the frequency-doubled (475 nm) output of a mode-locked titanium−sapphire laser (pulse width of 2 ps) with an external pulse picker to reduce the repetition rate from 76 to 3.8 MHz. The emission was detected at 530 nm (16 nm bandwidth) under magic angle conditions using a microchannel plate photomultiplier (impulse response width of 35 ps). The decays were collected in 4096 channels with a time increment of 9 ps per channel.

For each ribozyme construct, two separate donor decays were recorded and analyzed. The first, obtained with a sample labeled with only the Fl donor, was fitted using a sum of exponential decays to yield the intrinsic donor lifetimes and corresponding decay amplitudes. The decay of the doubly labeled ribozyme−substrate complex was analyzed in terms of two distinct donor−acceptor distance distributions, corresponding to docked and extended conformers as described previously (*14*). Nonlinear least-squares fitting of the donor decay recovered the mean donor−acceptor distance for each conformer, as well as their fractional populations.

The equilibrium constant for docking, K_{dock}, the free energy difference between docked and extended conformers, ΔG_{dock}, and the destabilization, $\Delta\Delta G_{dock}$, due to a ribozyme modification were calculated as described previously (*8*).

The nonadditive effect of combining two mutations on the stability of the hairpin ribozyme was quantified in terms of the free energy term δ, defined in Figure 4 in the Results and Discussion. δ was calculated as follows (*15*):

$$\delta = \Delta G_{dock}(\text{double mutant}) - \Delta G_{dock}(\text{mutant1}) - \Delta G_{dock}(\text{mutant2}) + \Delta G_{dock}(\text{wild-type})$$

where positive values reflect a synergistic effect of the two mutations, negative values are due to partial additivity, no additional effect of mutation 2, or an antagonistic effect, and a δ of 0 reflects additivity.

RESULTS AND DISCUSSION

Hydrogen Bonds in U42 and G+1 Binding Pockets Stabilize the Docked 4WJ Hairpin Ribozyme. The hydrogen bonding networks surrounding U42 and G+1, observed in the crystal structure of the docked hairpin ribozyme (*7*), are illustrated in panels A and B of Figure 2, respectively. Since these networks connect nucleotides within loop A with those within loop B, each of the hydrogen bonds might contribute to the tertiary structure stability of the docked hairpin ribozyme. To quantify the energetic importance of each hydrogen bond, we have introduced into the ribozyme a series of nucleotide analogues (Figure 1B) that remove individual hydrogen bonds (numbered 1−10 in Figure 2), either singly or in various combinations, and quantified the resulting changes in the distribution of docked and extended conformers by means of trFRET analysis.

Table 1: Destabilization Energies of Singly Modified Hairpin Ribozymes

	H-bond(s) removed[a]	fraction docked	K_{dock}	ΔG_{dock} (kJ/mol)	$\Delta\Delta G_{dock}$ (kJ/mol)
		Wild-Type			
	0	0.93 ± 0.005	12.9 ± 0.9	−6.4 ± 0.2	0 ± 0.3
		G+1 Binding Pocket			
G+1A	1−3	0.75 ± 0.05	3.0 ± 0.6	−2.7 ± 0.5	3.7 ± 0.5
G+1Pur	1−3	0.81 ± 0.02	4.4 ± 0.5	−3.7 ± 0.3	2.7 ± 0.3
G+1−2-AP	1 and 2	0.86 ± 0.003	6.2 ± 0.2	−4.5 ± 0.07	1.8 ± 0.2
G+1I	3	0.86 ± 0.03	6.2 ± 1.2	−4.5 ± 0.5	1.8 ± 0.5
G+1dG	4	0.85 ± 0.01	5.7 ± 0.4	−4.3 ± 0.2	2.1 ± 0.2
G8I	5	0.85 ± 0.01	5.5 ± 0.5	−4.2 ± 0.2	2.1 ± 0.3
		U42 Binding Pocket			
U42C	8−10	0.80 ± 0.003	3.9 ± 0.4	−3.4 ± 0.2	3.0 ± 0.2
A23Pur	9	0.84 ± 0.03	5.4 ± 0.1	−4.2 ± 0.04	2.2 ± 0.4
A23I	8 and 9	0.73 ± 0.05	2.6 ± 0.5	−2.4 ± 0.5	3.9 ± 0.3
A22Pur	7	0.88 ± 0.002	7.2 ± 0.1	−4.9 ± 0.05	1.5 ± 0.2
dU12	6	0.84 ± 0.003	5.2 ± 0.1	−4.1 ± 0.04	2.2 ± 0.2
G11I	10	0.87 ± 0.005	6.6 ± 0.3	−4.7 ± 0.1	1.7 ± 0.2

[a] For the numbering scheme, see Figure 2.

Analysis of the time-resolved fluorescence decay profiles of the fluorescein donor (attached to the end of the loop A domain) in the presence of the tetramethylrhodamine acceptor (attached to the end of the loop B domain) (Figure 3A) yielded the average donor−acceptor distance for the docked and extended ribozyme conformers, as well as the equilibrium fractions of each species. The donor−acceptor distances obtained for the docked conformers were constant within the range of 35−39 Å among all modified ribozymes. When the lengths of the helical arms carrying the fluorophores are taken into account, this range in interfluorophore distances translates into only a slight variation in the interhelical angles by <2−3°, indicating that the global structure of the docked ribozymes was not significantly perturbed in any of the modified ribozymes. However, compared to the wild type, the fraction of the docked species was reduced in all modified ribozymes, indicating that the nucleotide substitutions interfere with docking.

In accord with the crystal structure, removal of any hydrogen bond within the U42 or G+1 binding pockets destabilizes the docked ribozyme (Table 1). The most destabilizing modifications are G+1A and A23I (Table 1), each of which disrupts a Watson−Crick base pair in either the G+1 or U42 pocket (Figure 2A,B). Previous evidence for the G+1·C25 base pair was inferred from the compensatory effect of base changes at positions +1 and 25 on the catalytic activity of the hairpin ribozyme (*16*). Consistent with our results, a former ssFRET study showed significant destabilization of a G+1A ribozyme (*17*), and trFRET data showed a significant destabilization of G+1A variants of 2WJ and 4WJ ribozymes (*13*).

Energetic Contributions of Tertiary Hydrogen Bonds. The results presented above indicate that each of the hydrogen

Table 2: Destabilization Energies of Hairpin Ribozymes Containing Multiple Modifications

	H-bonds removed[a]	fraction docked	K_{dock}	ΔG_{dock} (kJ/mol)	$\Delta\Delta G_{dock}$ (kJ/mol)	$\Delta\Delta G_{dock}$ (additive)[b] (kJ/mol)
One Modification in Each Pocket						
G+1A/U42C	1−3 and 8−10	0.47 ± 0.01	0.9 ± 0.03	0.3 ± 0.1	6.6 ± 0.2	6.7 ± 0.6
G+1Pur/U42C	1−3 and 8−10	0.55 ± 0.01	1.2 ± 0.04	−0.5 ± 0.1	5.8 ± 0.2	5.7 ± 0.4
G+1dG/dU12	4 and 6	0.75 ± 0.01	3.0 ± 0.2	−2.8 ± 0.1	3.6 ± 0.2	4.3 ± 0.3
G+1A/dU12	1−3 and 6	0.63 ± 0.01	1.67 ± 0.06	−1.3 ± 0.1	5.1 ± 0.2	5.9 ± 0.6
Two or More Modifications in the G+1 Pocket						
G+1dA	1−4	0.69 ± 0.005	2.2 ± 0.04	−2.0 ± 0.04	4.4 ± 0.2	5.7 ± 0.3
G+1A/G8I	1−3 and 5	0.78 ± 0.02	3.5 ± 0.26	−3.1 ± 0.2	3.2 ± 0.3	5.8 ± 0.6
G+1dG/G8I	4 and 5	0.78 ± 0.03	3.6 ± 0.5	−3.2 ± 0.4	3.2 ± 0.4	4.2 ± 0.4
G+1I/G8I	3 and 5	0.81 ± 0.01	4.3 ± 0.4	−3.6 ± 0.2	2.7 ± 0.3	3.9 ± 0.6
G+1dA/G8I	1−5	0.72 ± 0.01	2.5 ± 0.1	−2.3 ± 0.1	4.1 ± 0.2	7.8 ± 0.6
Two Modifications in the U42 Pocket						
dU12/U42C	6 and 8−10	0.74 ± 0.01	2.8 ± 0.1	−2.6 ± 0.1	3.8 ± 0.2	5.2 ± 0.3
A23I/U42C	8−10	0.69 ± 0.01	2.2 ± 0.1	−2.0 ± 0.1	4.4 ± 0.2	6.9 ± 0.2
Two or More Modifications in the U42 Pocket and One or More Modifications in the G+1 Pocket						
G+1A/dU12/U42C	1−3, 6, and 8−10	0.43 ± 0.05	0.8 ± 0.1	0.7 ± 0.4	7.1 ± 0.4	8.9 ± 0.6
G8I/dU12/A22Pur	5−7	0.75 ± 0.002	3.0 ± 0.03	−2.7 ± 0.02	3.7 ± 0.2	5.8 ± 0.7
G8I/dU12/A22Pur/U42C	5−10	0.63 ± 0.007	1.7 ± 0.04	−1.3 ± 0.06	5.0 ± 0.2	8.8 ± 0.4
G+1dA/G8I/dU12/A22Pur/U42C	1−10	0.57 ± 0.003	1.3 ± 0.01	−0.7 ± 0.02	5.7 ± 0.2	14.5 ± 0.5

[a] For the numbering scheme, see Figure 2. [b] Values are the sums of single modifications.

bonds identified in the crystal structure contributes to the tertiary structure stability of the docked ribozyme. These contributions were quantified from analysis of the docking equilibrium in each of the ribozyme variants. From the fractional populations of docked and extended conformers obtained from the analysis of donor fluorescence decays, the equilibrium constants for docking, K_{dock}, as well as the free energy differences between docked and extended conformers, ΔG_{dock}, and the differences in free energy relative to that of the wild-type, $\Delta\Delta G_{dock}$, were calculated (Table 1).

The G+1I, G+1dG, and G8I substitutions remove hydrogen bonds 3, 4 or 5 from the G+1 pocket, respectively (Figures 1B and 2A), in each case destabilizing the docked ribozyme by ∼2 kJ/mol (Table 1). Similarly, the dU12, A22Pur, A23Pur, and G11I substitutions eliminate hydrogen bonds 6, 7, 9, and 10 from the U42 pocket, respectively (Figures 1B and 2B), again causing a destabilization of ∼2 kJ/mol in each case (Table 1). Since only a single hydrogen bond is removed in these variants, the four remaining hydrogen bonds restrict the conformational flexibility of bases within the G+1 or U42 pocket, preventing the formation of compensatory interactions that might otherwise obscure the energetic impact of the hydrogen bond that is being removed. Moreover, the nonspecific destabilization resulting from a single nucleotide modification is significantly less than 2 kJ/mol. For example, replacing an A with Pur at a position not involved in hydrogen bonds [A10Pur (*18*)] destabilizes the 2WJ ribozyme by only 0.6 kJ/mol, a value which is expected to be even smaller in the 4WJ ribozyme. Thus, the tertiary structure destabilization observed for the variants described above can be attributed to the loss of the specific hydrogen bond that is being removed. Our results consistently show that the energetic contribution of a single tertiary hydrogen bond is ∼2 kJ/mol, which is virtually identical to the contribution per hydrogen bond in the *Tetrahymena* ribozyme ribose zipper (*19*). This agreement provides confidence in our ability to quantify tertiary interaction energies by means of trFRET analysis of the docked and extended conformer populations in modified ribozymes.

With the exception of the A23I variant, nucleotide modifications that disrupt two or more Watson−Crick hydrogen bonds in the U42 (U42C) or G+1 (G+1A, G+1Pur, or G+1−2-AP) pockets are less destabilizing than expected on the basis of the number of hydrogen bonds that are being removed (Table 1). In these variants, the removal of multiple Watson−Crick hydrogen bonds could result in local conformational rearrangements that allow for the formation of compensatory interactions. For example, in the G+1−2-AP variant, a shift in the relative position of the 2AP+1 and C25 bases would allow for the formation of a wobble base pair with two hydrogen bonds (between the exocyclic amine of C25 and N1 of 2-AP and between N3 of C25 and N2 of 2-AP). The net effect of the rearrangement would be the loss of just a single hydrogen bond, which is consistent with the destabilization observed for the G+1−2-AP variant (Table 1). Similarly, in the G+1Pur and G+1A variants, retention of one hydrogen bond (between N3 in C25 and the exocyclic amine of A and between the exocyclic amine of C25 and N1 in Pur, respectively) would become possible through such a shift in position. A similar rearrangement within the U42 pocket, with retention of a single hydrogen bond (between the exocyclic amine of C42 and N1 of A23), could partially compensate for the loss of hydrogen bonds 8−10 in the U42C variant (Table 1).

The U42 and G+1 Binding Pockets Are Energetically Independent. The crystal structure of the docked hairpin ribozyme indicates that the G+1 and U42 binding pockets are physically distinct (*7*). Accordingly, interactions in different binding pockets should be independent of each other. To confirm this independence, we examined double-mutant ribozymes containing a single substitution in each binding pocket (G+1A/U42C, G+1Pur/U42C, G+1dG/dU12, and G+1A/dU12). As expected, the destabilization of these double mutants is equal, within the experimental error, to the sum of the destabilization energies of the corresponding single mutants (Figure 3B and Table 2). These results confirm that interactions within the U42 pocket are independent of those within the G+1 pocket, and that no

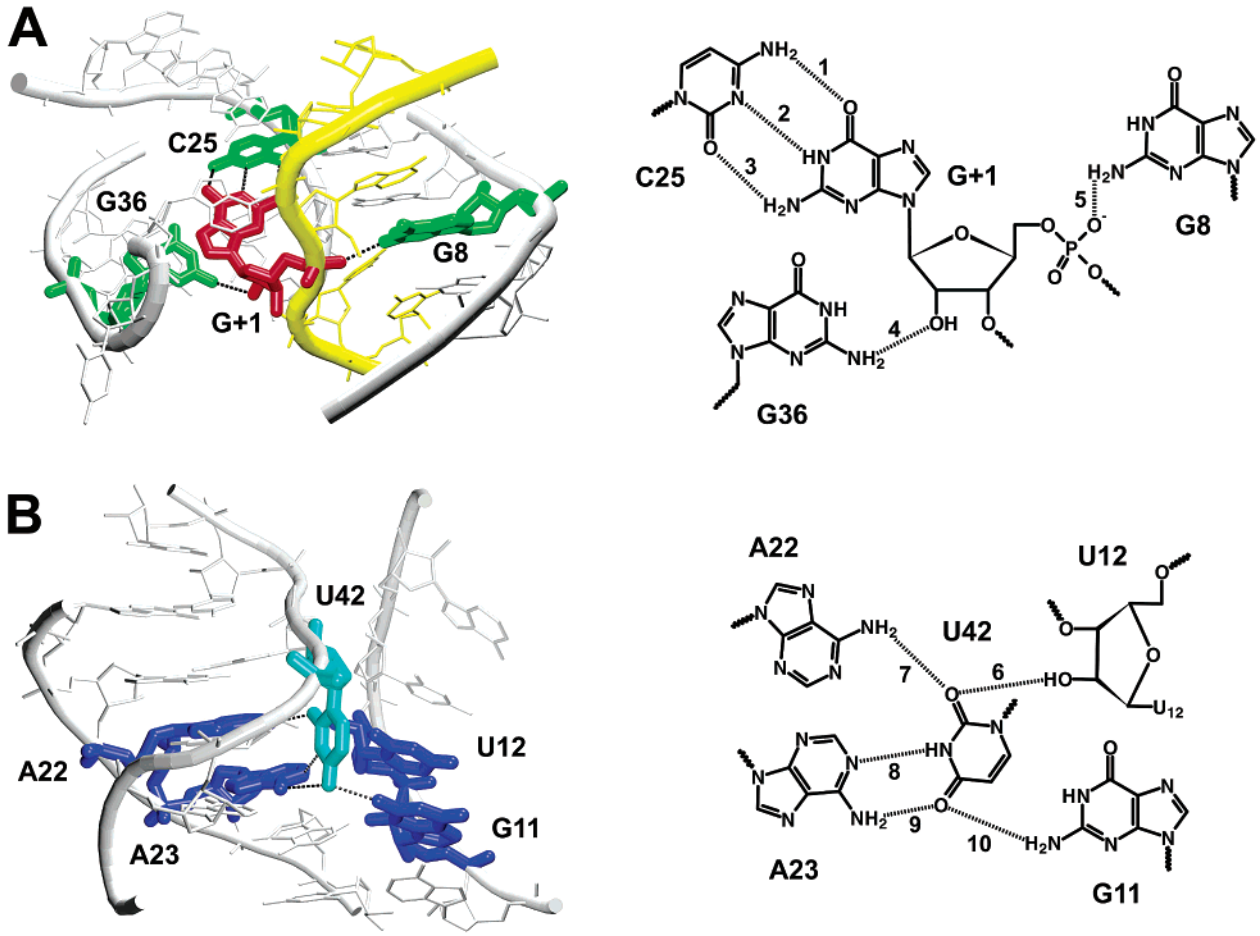

FIGURE 2: Hydrogen bonding interactions in the G+1 and U42 binding pockets. (A) Structural view of the G+1 pocket (left panel) and schematic representation of the hydrogen bonding pattern with numbering scheme used in the text (right panel). G+1 forms a Watson−Crick base pair with C25 (loop B, hydrogen bonds 1−3) and hydrogen bonds via its 2′-OH group with the exocyclic amino group of G36 (loop B, hydrogen bond 4) and via the 5′-phosphate with the exocyclic amino group of G8 (loop A, hydrogen bond 5). In the left panel, G+1 is shown in red, G8, C25, and G36 are shown in green, and the substrate strand is depicted in yellow. (B) Structural view of the U42 pocket (left panel) and schematic representation of the hydrogen bonding pattern (right panel). U42 (cyan) points into a binding pocket formed by G11, U12, A22, and A23 (blue) and forms a Watson−Crick base pair with A23 (loop B, hydrogen bonds 8 and 9). U42 also hydrogen bonds via O4 with the exocyclic amino group of G11 (loop A, hydrogen bond 10) and via O2 with both the 2′-hydroxyl of U12 (loop A, hydrogen bond 6) and the exocyclic amino group of A22 (loop B, hydrogen bond 7). The structures were generated with VMD (*23*) and rendered using Raster3D (*24*). The PDB entry is 1HP6 (*7*).

compensatory interactions are formed in the double-mutant ribozymes.

Energetic Coupling within the G+1 and U42 Binding Pockets. The structure of the G+1 binding pocket suggests that interactions within the pocket are interdependent. The G+1·C25 base pair fixes the guanine base and restrains the ribose pucker to 2′-endo (*7*). This most likely restricts the local backbone flexibility, thereby affecting hydrogen bonds 4 and 5 that involve ribose and phosphate, and vice versa (Figure 2A). Similar coupling mechanisms may exist in the U42 pocket (Figure 2B). To investigate possible cooperativity between hydrogen bonds, we examined hairpin ribozymes containing two or more substitutions within the G+1 or U42 pocket (Table 2). In each of the double mutants that was examined, the destabilization of the docked ribozyme was consistently less than expected from the additive effect of the two single mutations (Figure 3B).

The docking energetics of the double-mutant ribozymes and each of the corresponding single mutants can be represented as a thermodynamic cycle, as shown in Figure 4 (*20*). Here, R_{00} represents the wild-type ribozyme (actually the ribozyme−substrate complex), and R_{i0} and R_{0j} represent single-base changes at sites *i* and *j*, respectively. The free energies ΔG_i and ΔG_j represent the energetic cost of introducing the mutations at the respective sites. R_{ij} represents the double-mutant ribozyme with base changes at both sites. The upper part of the cycle represents the free energy change incurred when a mutation at site *j* is introduced into a ribozyme that also contains a mutation at site *i*. Likewise, the right-hand side of the cycle depicts the introduction of a mutation at site *i* in the background of a mutation at site *j*. The differential destabilization of a second mutation in the presence of the first is denoted by a free energy δ. The δ values for each double-mutant ribozyme were calculated as described in Experimental Procedures and are listed in Table 3. Each of the δ values is negative, showing that the energetic impact of a given mutation is lessened in the presence of a second mutation. It is important to note that δ is defined thermodynamically and is independent of the mechanism responsible for nonadditivity.

The results for a complete triple-mutant cycle within the G+1 pocket can be represented in the form of a cube (Figure 5), where each face of the cube corresponds to a thermodynamic cycle. For example, the front fact shows the effect

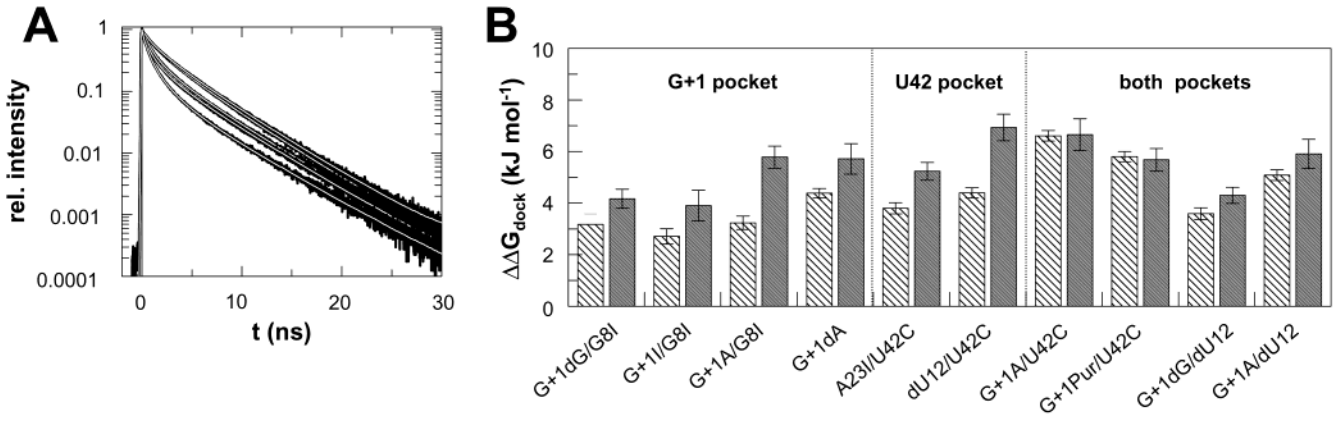

FIGURE 3: Effect of ribozyme modifications on docking as determined from trFRET analysis. (A) Donor fluorescence decays in the presence of an acceptor fluorophore for wild-type and selected modified ribozymes. Shown are (from top to bottom) donor decays (black) for G+1A/U42C (47% docked), G+1dA/G8I/dU12/A22Pur/U42C (57% docked), G+1A (75% docked), U42C (78% docked), and the wild-type ribozyme (93% docked) together with the corresponding distance fits (white lines). The time-resolved fluorescence decays of the donor of the Fl-TMR-labeled ribozymes were analyzed in terms of two distance distributions, reflecting the extended and docked conformers of the ribozyme−substrate complex. From all fits, two distance distributions centered around 35 (docked conformer) and 70 Å (extended conformer) were extracted. These fits converged to reduced χ^2 values between 1.1 and 1.2. (B) Destabilization energies of doubly-modified ribozymes. $\Delta\Delta G_{dock}$ values determined from trFRET (cross hatched) and calculated from single mutants assuming additivity (gray) are shown for double modifications within the G+1 pocket, within the U42 pocket, or for double modifications affecting both pockets. The error bars reflect the deviations of the individual docked fractions in two independent trFRET experiments from the mean value, which have been propagated to $\Delta\Delta G_{dock}$ as described previously (*8*).

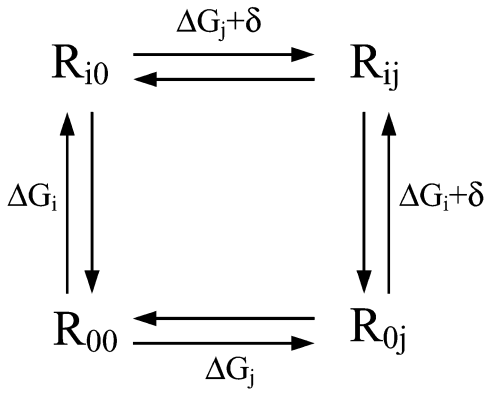

FIGURE 4: Thermodynamic cycle used to represent the energetic coupling of two mutations in the G+1 or U42 pocket. R_{00} represents the wild-type ribozyme, while R_{i0} and R_{0j} represent single-base changes at sites *i* and *j*, respectively. The energetic costs for the introduction of these mutations are ΔG_i and ΔG_j. R_{ij} is the double-mutant ribozyme in which changes at both sites are introduced simultaneously. The top left half of the cycle shows the consecutive introduction of mutations at sites *i* and *j*, while the bottom right half shows the consecutive introduction of mutations at sites *j* and *i*. The free energy term δ (see Experimental Procedures) reflects the difference in the destabilizing effect of two mutations introduced at the same time (R_{ij}) compared to the sum of the effects of each individual mutation (R_{i0} and R_{0j}). A δ value of 0 is obtained for additive effects of two mutations.

of combining the G+1 and G+1dG mutations in the background of the wild-type ribozyme. The back face shows the effect of combining these same mutations in the background of a third mutation, G8I in this case. The δ values for each pair of mutations, in the background of a third mutation (denoted with a superscript 1), are given in Table 3. Interestingly, the nonadditive effect of combining a particular pair of mutations is diminished or eliminated in the presence of a third mutation (Table 3).

The nonadditive effect of two mutations may reflect cooperativity among individual interactions, as suggested by the structure of the G+1 pocket. Alternatively, the double-mutant variant may rearrange to form new, compensatory

Table 3: Nonadditivity of Tandem Mutations

	$^0\delta^a$ (kJ/mol)	$^1\delta^a$ (kJ/mol)
G+1dA	−1.3 ± 0.4	−0.2 ± 0.4
G+1A/G8I	−2.6 ± 0.6	−1.4 ± 0.6
G8I/G+1dG	−1.0 ± 0.4	0.1 ± 0.4
G+1I/G8I	−1.2 ± 0.7	
dU12/U42C	−1.4 ± 0.4	

[a] δ values are calculated as described in Experimental Procedures. The superscripts 0 and 1 refer to the wild-type background and the presence of a third mutation, respectively.

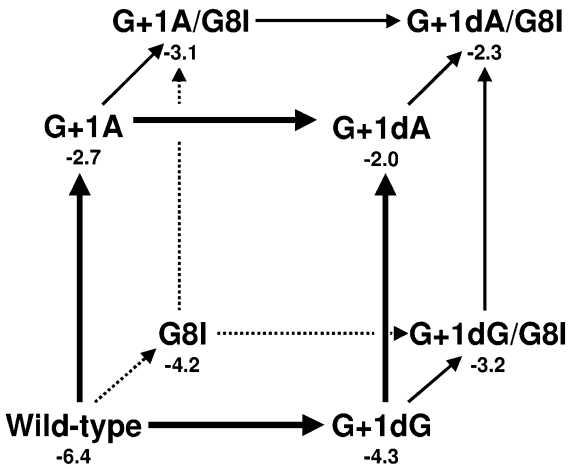

FIGURE 5: Thermodynamic analysis of the G+1 pocket. Cube representing the triple-mutant cycle for the G+1A, G8I, and G+1dG modifications. The numbers next to the modifications are the ΔG_{dock} values in kilojoules per mole. Each face of the cube represents a double-mutant cycle. As an example, the double-mutant cycle for the G+1A and G+1dG mutations is highlighted (front face, bold arrows). The directions of the arrows indicate the stepwise movement from the wild-type ribozyme (bottom left corner) to a mutant lacking all hydrogen bonds in the G+1 pocket (top right corner).

interactions. While the recovered donor−acceptor distances indicate that there is no significant change in the global structure of any of the ribozyme variants, we cannot rule

out the possibility of localized conformational changes at the docking interface. In fact, removal of all three Watson−Crick hydrogen bonds (hydrogen bonds 1−3, Figure 2A) in the G+1A mutant could allow the +1 base to wobble, with possible formation of compensatory hydrogen bonds, as discussed above. This may explain the nonadditivity of the G+1A and G8I, or G+1A and G+1dG, mutations. However, there is no evidence for the formation of compensatory interactions when a single hydrogen bond (3, 4, or 5) is removed (see above). Notably, the +1 base is likely to remain fixed. While it is possible, in principle, that some reorganization occurs when two of these hydrogen bonds are removed, cooperativity among the hydrogen bonds provides a simpler explanation for the observed nonadditivity of the G8I/G+1dG and G+1I/G8I double mutants. Thus, once a single element is removed from the hydrogen bond network, with the consequent loss of cooperative interaction energy, a second element can be removed with a smaller energetic penalty. This model also explains why the G8I and G+1dG mutations are additive in the presence of a third mutation. Ultimately, high-resolution structural information will be required to determine whether new interaction networks are formed in the ribozyme variants examined here. However, in the absence of such information, cooperative interactions among hydrogen bonds 3, 4 and 5 (at least) within the G+1 pocket provide the simplest explanation for the results presented here. These results emphasize the importance of energetically coupled hydrogen bond networks in RNA tertiary structure and show that energetic contributions of individual interactions derived from single mutants do not necessarily represent the complete thermodynamic picture.

Significant nonadditivity was also observed for ribozymes with two mutations in the U42 pocket (Table 2 and Figure 3B). In the case of the A23I/U42C variant, the nonadditivity is expected because both mutations affect the same interactions (hydrogen bonds 8 and 9, Figure 2B). In the dU12/U42C variant, the two mutations affect different interactions, suggesting possible cooperativity between the Watson−Crick base pair hydrogen bonds (hydrogen bonds 8 and 9) and hydrogen bonds 6 and 10. However, it is difficult to assess whether these hydrogen bonds are cooperatively coupled because there is evidence from the U42C single mutant that compensatory interactions may be formed upon removal of hydrogen bonds 8−10 (see above).

The U42 and G+1 Binding Pockets Constitute the Major Determinants for Tertiary Structure Stability. The results described above indicate that each of the hydrogen bonds surrounding G+1 or U42 contribute to the thermodynamic stability of the docked hairpin ribozyme. Thus, these interaction networks appear to be the major determinants of the tertiary structure stability. To investigate the effect of elimination of all 10 hydrogen bonds in both pockets, the docking equilibrium of a G+1dA/G8I (G+1 pocket) and U42C/A22Pur/dU12 (U42 pocket) variant was studied. Summing the effects of the five single modifications, one would expect a destabilization by ∼14 kJ/mol, resulting in as little as 5% docked conformer in equilibrium. However, a more realistic estimate must take into account the nonadditive effect of multiple mutations within each pocket. A G+1dA/G8I variant in which all hydrogen bonds are eliminated from the G+1 pocket indicates that the net destabilization is 4.1 kJ/mol (Table 2). Similarly, a G8I/dU12/A22Pur/U42C variant eliminates all interactions in the U42 pocket, plus hydrogen bond 5 in the G+1 pocket. This variant destabilizes docking by 5.0 kJ/mol (Table 2). Since the G+1 and U42 pockets are independent, a correction for the G8I substitution (2.1 kJ/mol) suggests that the net destabilization upon elimination of all interactions in the U42 pocket is 2.9 kJ/mol. Thus, when the nonadditive mutational effects are taken into account, the removal of all 10 hydrogen bonds from the G+1 and U42 pockets is expected to destabilize the docked ribozyme by ∼7 kJ/mol (4.1 + 2.9 kJ/mol). Consistent with this, docking of the G+1dA/G8I/dU12/A22Pur/U42C variant lacking all 10 hydrogen bonds is destabilized by 5.7 kJ/mol (Table 2).

Even though the removal of all hydrogen bonds from each pocket is less destabilizing than expected on the basis of additivity of single mutations, it is apparent that the G+1dA/G8I/dU12/A22Pur/U42C ribozyme retains only a marginal stability of the docked conformer ($\Delta G_{dock} = -0.7$ kJ/mol), indicating that favorable and unfavorable interactions are balanced. This clearly shows that G+1 and U42 are the major determinants of the thermodynamic stability of the tertiary structure in the 4WJ hairpin ribozyme, and explains why no significant contribution could be detected for the ribose zipper (*8*). In the NMR structure of the isolated loop A region, which presumably depicts the undocked ribozyme structure, G+1 is stacked within the distorted helix and forms a sheared base pair with A9 (*21*). Similarly, in the NMR structure of the isolated loop B domain, U42 forms a reverse Hoogsteen base pair with A22, while A23 interacts with A40 (*22*). Our findings suggest that the looping-out of G+1 and the resulting orientation of the G+1 base, ribose, and phosphate, as well as the rearrangement of U42, A22, and A23 and its interactions with U12 and G11, allow for an intricate network of hydrogen bonds in the docked hairpin ribozyme that is crucial for its stability.

ACKNOWLEDGMENT

We thank Sean Ryder and Markus Rudolph for helpful comments on the manuscript.

REFERENCES

1. Hermann, T., and Patel, D. J. (1999) *J. Mol. Biol. 294*, 829−849.
2. Fedor, M. J. (2000) *J. Mol. Biol. 297*, 269−291.
3. Feldstein, P. A., and Bruening, G. (1993) *Nucleic Acids Res. 21*, 1991−1998.
4. Komatsu, Y., Koizumi, M., Nakamura, H., and Ohtsuka, E. (1994) *J. Am. Chem. Soc. 116*, 3692−3696.
5. Earnshaw, D. J., Masquida, B., Muller, S., Sigurdsson, S. T., Eckstein, F., Westhof, E., and Gait, M. J. (1997) *J. Mol. Biol. 274*, 197−212.
6. Pinard, R., Heckman, J. E., and Burke, J. M. (1999) *J. Mol. Biol. 287*, 239−251.
7. Rupert, P. B., and Ferre-D'Amare, A. R. (2001) *Nature 410*, 780−786.
8. Klostermeier, D., and Millar, D. P. (2001) *Biochemistry 40*, 11211−11218.
9. Chowrira, B. M., Berzal-Herranz, A., Keller, C. F., and Burke, J. M. (1993) *J. Biol. Chem. 268*, 19458−19462.
10. Ryder, S. P., and Strobel, S. A. (1999) *J. Mol. Biol. 291*, 295−311.
11. Walter, N. G., Hampel, K. J., Brown, K. M., and Burke, J. M. (1998) *EMBO J. 17*, 2378−2391.
12. Earnshaw, D. J., Hamm, M. L., Piccirilli, J. A., Karpeisky, A., Beigelman, L., Ross, B. S., Manoharan, M., and Gait, M. J. (2000) *Biochemistry 39*, 6410−6421.

13. Walter, N. G., Burke, J. M., and Millar, D. P. (1999) *Nat. Struct. Biol. 6*, 544−549.
14. Eis, P. S., and Millar, D. P. (1993) *Biochemistry 32*, 13852−13860.
15. Horovitz, A., and Fersht, A. R. (1990) *J. Mol. Biol. 214*, 613−617.
16. Pinard, R., Lambert, D., Walter, N. G., Heckman, J. E., Major, F., and Burke, J. M. (1999) *Biochemistry 38*, 16035−16039.
17. Wilson, T. J., Zhao, Z. Y., Maxwell, K., Kontogiannis, L., and Lilley, D. M. (2001) *Biochemistry 40*, 2291−2302.
18. Ryder, S. P., Adegboyega, K. O., Padilla, J., Klostermeier, D., Millar, D. P., and Strobel, S. A. (2001) *RNA 7*, 1454−1463.
19. Silverman, S. K., and Cech, T. R. (1999) *Biochemistry 38*, 8691−8702.
20. di Cera, E. (1998) *Adv. Protein Chem. 51*, 59−119.
21. Cai, Z., and Tinoco, I., Jr. (1996) *Biochemistry 35*, 6026−6036.
22. Butcher, S. E., Allain, F. H., and Feigon, J. (1999) *Nat. Struct. Biol. 6*, 212−216.
23. Humphrey, W., Dahlke, A., and Schulten, K. (1996) *J. Mol. Graphics 14*, 33−38.
24. Merritt, A. E., and Bacon, D. J. (1997) *Methods Enzymol. 277*, 505−524.

BI025551B